J Mol Model (2013) 19:1727–1737
DOI 10.1007/s00894-012-1715-6

ORIGINAL PAPER

Theoretical investigation on ruthenium tetraazaporphyrin as potential nitric oxide carrier in biological systems

José M. M. Lima · Valter H. C. Silva · Lilian T. F. M. Camargo · Heibbe C. B. de Oliveira · Ademir J. Camargo

Received: 24 April 2012 / Accepted: 27 November 2012 / Published online: 8 January 2013

Abstract Nitric oxide (NO) is an important chemical compound involved in many physiological and pathological processes in living organisms. However, nitric oxide is a very reactive radical that needs to be carried through organisms to reach the desired biological target. With the aim of developing new compounds that can be used as biomedical NO carrier agents we carried out a theoretical investigation at B3LYP/6-31+G(d)/LANL2DZ level on the interaction of NO with RuTAP (Ruthenium tetraazaporphyrin) and Ru(L)TAP, where L=Cl^-, NH_3, and Pyridine (Py)) and the oxidation state of Ru ranging from +1 to +3. The theoretical calculation results show that the geometric and electronic parameters of the Ru–NO bond are highly dependent on the oxidation state of Ru and of the chemical nature of ligand L at axial position. The results also show clearly that RuTAP and Ru(L)TAP are good potential candidates to be used as NO carriers in living organisms.

Keywords Ruthenium tetraazaporphyrin · RuTAP · Nitric Oxide carrier · Porphyrazines · B3LYP

J. M. M. Lima · V. H. C. Silva · L. T. F. M. Camargo · A. J. Camargo (✉)
Unidade Universitária de Ciências Exatas e Tecnológicas, Universidade Estadual de Goiás, P.O. Box 459, 75001-970, Anápolis, GO, Brazil
e-mail: ajc@ueg.br

V. H. C. Silva · H. C. B. de Oliveira (✉)
Instituto de Química, Universidade de Brasília, 70919-970, Brasília, DF, Brazil
e-mail: heibbe@unb.br

Introduction

Under normal conditions of pressure and temperature, nitric oxide (NO) is a colorless gas that has low solubility in water, similar to nitrogen, oxygen, and carbon monoxide [1, 2]. In biological systems, a low level of NO production is widely known as an important molecule that helps regulate blood pressure, can act as a neurotransmitter and also acts on the immune system by helping to kill cancer cells and intracellular parasites such as *Trypanosoma*, *Plasmodium*, and *Leishmania* [3–10]. In living organisms, nitric oxide can be synthesized in vascular endothelial cells from the amino acid L-arginine by the catalytic action of the enzyme nitric oxide synthase [11, 12]. As a neurotransmitter, nitric oxide has interesting features, such as being produced in a specific area of the synaptic vesicles, and it does not need specific receptors. Furchpott & Zawadzki [13] showed that nitric oxide acts as a chemical messenger in the dilatation of blood vessels in blood pressure regulation. Finally, there has been an interesting discovery that nitric oxide acts on the immune system as an activator of macrophages [14].

Nitric oxide is an uncharged radical with a very low polarity of 0.157D [15]. It is very reactive and might react fundamentally with other free radicals, such as oxygen, to form nitrogen dioxide (NO_2), a toxic brown gas, and with all transition metals to form metal nitrosyl complexes. Its high reactivity rate helps to explain the short half-life for the endothelium-derived relaxing factor [16]. In view of the chemical behavior of nitric oxide, coordination complexes of iron, cobalt, chromium, and ruthenium with NO ligand have been widely investigated to develop molecular devices for releasing nitric oxide in target processes [17–21]. Therefore, our theoretical laboratory is interested in studying

molecular systems that can be used as potential nitric oxide carriers.

Our attention was drawn to ruthenium complexes because they exhibit three important features for our purpose: rate of ligand substitution, several oxidation states that are accessible to biological systems, and the ability of ruthenium to mimic iron in forming chemical bonds with some biological molecules [22]. In addition, ruthenium complexes have high chemical, electrochemical, geometrical and enantiomeric stability [23]. These properties are very important characteristics for a metal to be used as a drug, because it needs to reach the biological target without being chemically modified. It is also important to consider the fact that the rate of ligand substitution is highly dependent on the ligand concentration in the nearby solution. Diseases that modify the ligand concentration in cells or in the adjacent tissues might produce an effect on drug activity. Most drugs interact with proteins or with small molecules like water molecules, for example. Some interactions are important for the desired therapeutic effect of the complexes.

Another important feature of ruthenium is that its oxidation states +1, +2, and +3 are all accessible under physiological conditions [22]. In these oxidation states the ruthenium atom is essentially hexacoordinate with octahedral geometry, and Ru^{3+} complexes are more biologically inert than the Ru^{1+} and Ru^{2+} complexes. The redox potential of a complex can be modified, for example, by varying the complex ligands [24, 25]. In biological systems glutathione, ascorbate and single electron transfer proteins are biological reducers and they are able to reduce Ru^{3+} and Ru^{2+}, while oxygen and cytochrome oxidase can oxidize Ru^{2+} [22]. Therefore, the redox potential of ruthenium compounds can be used to improve the efficacy of drugs in disease treatment. For example, the drug can be administered as relatively inert Ru^{3+} complexes, which are activated by reduction in diseased tissues.

Furthermore, in many cases the modified metabolisms associated with diseases such as cancers and infections result in lower oxygen concentration in the tissues, promoting a reductive environment. Cancer cells are known to have higher levels of glutathione and a lower pH than healthy tissues, creating a strongly reducing environment [22]. If the active Ru^{2+} complex leaves the low oxygen environment, it may be converted back to Ru^{3+} by a variety of biological oxidants. The low toxicity of ruthenium complexes is probably related to the ability of ruthenium to mimic iron in binding to many biomolecules, including serum transferrin and albumin, which are responsible for transporting iron. It is well known that cells infected by parasites or cancerous cells divide rapidly and they have a greater demand for iron, increasing the number of transferring receptors located on their surfaces. As ruthenium mimics iron, nitrosyl ruthenium complexes might be rapidly captured by these cells and in turn deliver nitric oxide inside or near targeted cells and thus eliminate the diseased cells.

In this study, the ruthenium atom is coordinated with tetraazaporphyrin to form the ruthenium tetraazaporphyrin (RuTAP) complex. For a molecule to be used as a nitric oxide carrier in biological systems it is very important to remember that nitric oxide's binding strength to RuTAP will depend on that molecule's oxidation states, i.e., the Ru–NO bond should be stronger in some oxidation states and weaker in others. It is also important to know that the geometric and electronic parameters of the Ru–NO bond depend on the L ligand at axial position, which provides a greater degree of freedom to design an NO carrier for a specific target. The aim of this work was to study theoretically the interaction between nitric oxide and RuTAP and Ru(L)TAP for the +1, +2, and +3 oxidation states of Ru to see if Ru(NO)TAP and Ru(NO)(L)TAP ($L=Cl^-$, NH_3, or Py) can be used as NO carriers in biological systems.

This paper is organized as follows: in "Computational procedure" section we present the computational details carried out in this work. Analysis and discussion of results are presented in "Results and discussion" section. The final conclusions are shown in "Conclusions" section.

Computational procedure

The theoretical treatment of the systems included in this work was performed using the density functional theory (DFT) approach of the Gaussian 03 series of programs [26]. The atomic numbering used in the theoretical calculations for RuTAP and Ru(NO)TAP is shown in Fig. 1. The calculations reported in this work were carried out using the Kohn-Sham density functional theory (DFT) with Beck three-parameters hybrid exchange-correlation functional, known as B3LYP [27–29], and the 6-31+G(d)/LANL2DZ basis set (i.e. LANL2DZ pseudo potential for Ru and the 6-31+G(d) split-valence basis set for all other atoms). The local minimums on the potential energy hypersurface were characterized by the computation of the vibrational harmonic frequencies at the same level of theory used in the geometry optimizations. The absence of vibrational modes with imaginary frequencies shows that the optimized molecular geometries are at a local minimum on the potential energy hypersurface. Since the binding energies include a basis set superposition error (BSSE) [30, 31], due to the supermolecule approach, the full counterpoise method of Boys and Bernardi [32] was employed to estimate the BSSE, resulting in the corrected binding energy (ΔE^{corr}) values. All the bond order indexes were obtained from natural population analysis (NPA) using the NBO 3.1 [33–40] program. The atomic partial charges on the atoms were obtained from CHELPG (**CH**arges from **EL**ectrostatic **P**otentials using a

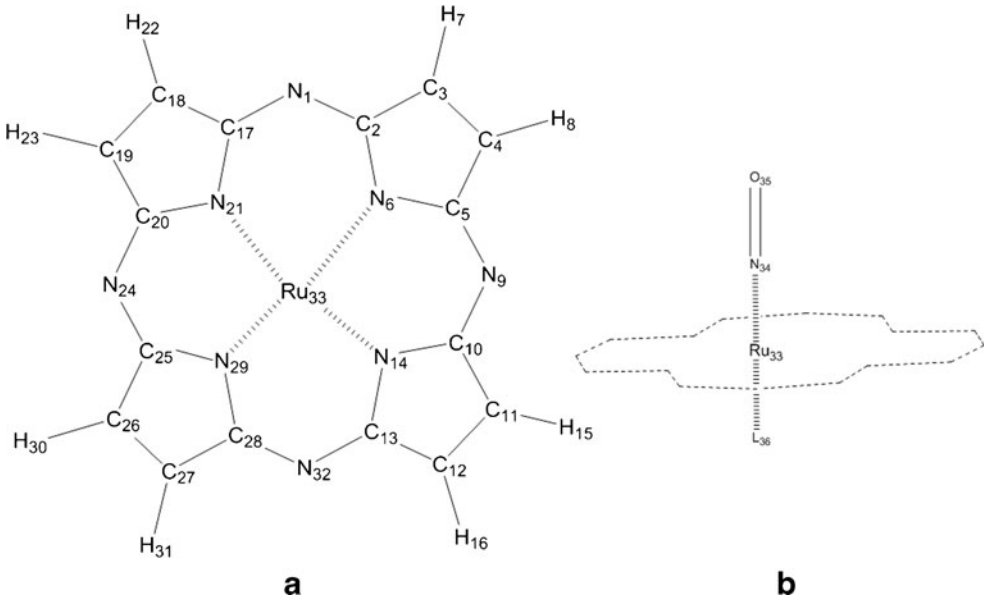

Fig. 1 Atomic numbering adopted in this work. The molecular plane is defined as the plane containing the tetraazaporphyrin ligand (TAP)

Grid based method) scheme by Breneman and Wiberg [41] at B3LYP/6-31+G(d)/LANL2DZ level.

Since zero-point vibrational energy (ZPVE) contributions have a non-negligible effect on the stabilities of NO group bonded to the RuTAP or Ru(L)TAP complexes, we have evaluated these contributions using the B3LYP/6-31+G(d)/LANL2DZ level of theory for nitric oxide complexed to them, i.e., Ru(NO)TAP and Ru(NO)(L)TAP for the +1, +2, and +3 oxidation states of Ru. The corrected binding energies for the complexes were calculated according to the following equation [42]:

$$\Delta E = \left[E(NORuTAP) + E(NORuTAP)_{ZPVE}\right] - \left[E(RuTAP)_{BSSE} + E(RuTAP)_{ZPVE} + E(NO)_{BSSE} + E(NO)_{ZPVE}\right]$$

where ΔE represents the interaction energy, E is the calculated energy at B3LYP/6-31+G(d)/LANL2DZ level for each species. The general reaction for the complex formation can be written in a general way as NO+Ru(L)TAP→ [(NO)Ru(L)TAP], where L stands for Cl^-, NH_3, and Py, and the oxidation states of Ru ranging from +1 to +3. Standard statistical mechanical formulae provide the enthalpy (ΔH) and Gibbs free energy (ΔG) adjustment from 0 K to 298.15 K [43].

Results and discussion

As mentioned before, the +1, +2, and +3 oxidation states of Ru are all accessible for ruthenium complexes in the biological systems. For this reason, our theoretical group decided to investigate the interaction between NO and RuTAP and Ru(L)TAP (L=Cl^-, NH_3, or Py) complexes for Ru oxidation states ranging from +1 to +3. The two acidic hydrogens inside the macrocycle of tetraazaporphyrin (TAP) are removed and TAP becomes a dianion. For example, if we are using the Ru atom in its +1 oxidation state, then the net charge on the RuTAP system will be −1: $[RuTAP]^{1-}$. The charges on the other complexes are obtained in the same way.

The use of different L ligands in the Ru(NO)(L)TAP complexes aimed to investigate the effect of the ligands on the geometric and electronic parameters of the Ru–NO bond.

RuTAP complex

The starting point of this investigation was to study the RuTAP complex. This is important for establishing if the coordination of NO to RuTAP significantly affects the geometrical and electronic parameters of RuTAP. The complexes to be studied were $[RuTAP]^{1-}$, $[RuTAP]^{0}$, and $[RuTAP]^{1+}$ for the +1, +2, and +3 oxidation states of Ru, respectively. The geometric parameters fully optimized at B3LYP/6-31+G(d)/LANL2DZ level for these complexes are shown in Table 1. The calculation results show that the RuTAP complex has symmetry D_{4h} in gas phase for all its oxidation states investigated, and the geometric parameters are also the same for all RuTAP complexes (Fig. 2a). The Ru–N_x (x=6, 14, 21, or 29) bond length (see Fig. 1 for the numbering used) is about 2.0 Å and the Ru atom is perfectly centered in the molecular plane.

The calculated Ru–N_x bond orders for RuTAP in the +1, +2, and +3 oxidation states of Ru are 0.463, 0.428, and 0.424, respectively. These values show that the bonds between Ru and N atoms from TAP can be considered as single bonds; increasing the oxidation state decreases the bond orders and in turn the bond strength. The calculated partial charges on the atoms derived from the CHELPG procedure at B3LYP/6-31+

Table 1 Bond lengths (Å) and bond angles (°) calculated for RuTAP and Ru(NO)TAP for the oxidation states of Ru ranging from +1 to +3 at the B3LYP/6-31+G(d)/LANL2DZ level

	Ru^{1+}		Ru^{2+}		Ru^{3+}	
	$[RuTAP]^{1-}$	$[(NO)RuTAP]^{1-}$	$[RuTAP]^{0}$	$[(NO)RuTAP]^{0}$	$[RuTAP]^{1+}$	$[(NO)RuTAP]^{1+}$
N6 – Ru	1.995	2.019	2.008	2.021	1.995	2.016
N14 – Ru	1.995	2.009	2.008	2.030	1.995	2.016
N21 – Ru	1.995	2.002	2.008	2.012	1.995	2.016
N29 – Ru	1.995	2.019	2.008	2.021	1.995	2.016
Ru – NO	———	1.923	———	1.827	———	1.728
Ru – plane	0.000	0.205	0.000	0.281	0.000	0.443
N – O	———	1.203	———	1.182	———	1.157
N21 –Ru– N14	180.0	168.3	180.0	164.0	180.0	155.2
Ru – N – O	———	122.1	———	140.9	———	180.0

G(d)/LANL2DZ level are shown in Table 2, and these are 0.49, 1.35, and 0.75 for the oxidation states +1, +2, and +3, respectively. The nature of these charges can be better understood from the analysis of the highest molecular orbital (HOMO) shown in Fig. 3a. The HOMO orbitals for the $[RuTAP]^{1-}$ and $[RuTAP]^{1+}$ complexes are spread out on the complex's macrocycle, including the region over the Ru atom, which helps to increase the electron density on Ru, making it less positive. However, the HOMO for $[RuTAP]^{0}$ is spread out on the TAP macrocycle only, i.e., this orbital does not have any contribution from the Ru atom. As a consequence, there is a decrease in the electron density in the Ru atom, making it in turn more positive for +2 oxidation state.

Interaction between NO and RuTAP

The Ru(NO)TAP geometric parameters fully optimized at B3LYP/6-31+G(d)/LANL2DZ level for the +1, +2, and +3 oxidation states of Ru are shown in Table 1. The calculation results show that the Ru–NO bond length in the (NO)RuTAP complex is strongly dependent on the oxidation state of Ru. The calculated Ru–NO bond lengths for $[Ru(NO)TAP]^{1-}$, $[Ru(NO)TAP]^{0}$, and $[Ru(NO)TAP]^{1+}$ complexes are 1.923 Å, 1.827 Å, and 1.728 Å, respectively. These lengths show that increasing the oxidation state of Ru by one unit makes the bond length decrease by about 5 %. This means that the Ru–NO bond is stronger for the +3 oxidation state and weaker for the +1 oxidation state of Ru. Another interesting observation is the projection of the Ru atom out of the molecular plane. When the NO group binds to the RuTAP to form the Ru(NO)TAP complex one can observe the projection of Ru out of the molecular plane for all three oxidation states of Ru. The calculated projections are 0.205 Å, 0.827 Å, and 0.443 Å for the +1, +2, and +3 oxidation states of Ru, respectively. As a consequence of these projections, the $Ru–N_x$ (x=6, 14, 21, or 29) bond lengths increase by about 1 %. The effects of changing the oxidation state on the projections of Ru are about 37 % when the oxidation state of Ru changes from +1 to +2 and about 58 % when the oxidation state of Ru changes from +2 to +3. The variation of the oxidation state of Ru also affects the N–O bond length of the nitric oxide group, as can be seen in Table 1. This bond length is longer for the +1 oxidation state and shorter for the +3 oxidation state. The variation is almost linear with the increase in oxidation state of Ru and is about 2 % from one state to another. The oxidation state of Ru does not affect the $Ru–N_x$ bond length. This means that these chemical bonds are stable under the oxidation processes studied here. The remaining TAP macrocycle geometric parameters are also unaffected by the oxidation process. This is a good result because we are using the TAP ligand to design a molecular carrier for the NO group, and it is important for the carrier to have chemical stability, especially to be stable under the reduction-oxidation processes in our case.

The data in Table 1 also show an influence of the oxidation state of Ru on the Ru–N–O angle. For the +3 state of Ru, the Ru–N–O angle is of 180° (see Fig. 2b), while for the +1 and +2 states of Ru the bending angles are 122.1 and 140.9°, respectively. The HOMO orbitals for these complexes are shown in Fig. 3b, and help to understand the variation of the Ru–N–O angle with the change in the oxidation state of Ru. For the +1 and +2 states of Ru the HOMO is a bonding orbital between Ru and N from the nitric oxide group. However, it is the p-type atomic orbital of N of the NO group that contributes to the HOMO formation. In order to improve the overlap of this orbital with the orbital from RuTAP the Ru–N–O angle must decrease. This angle is smaller for the +1 state of Ru than for the +2 state, since the HOMO is bigger between Ru and N of the NO group in the +1 state of Ru (see Fig. 2b). In the +3 oxidation state of Ru there is no HOMO orbital contribution in the

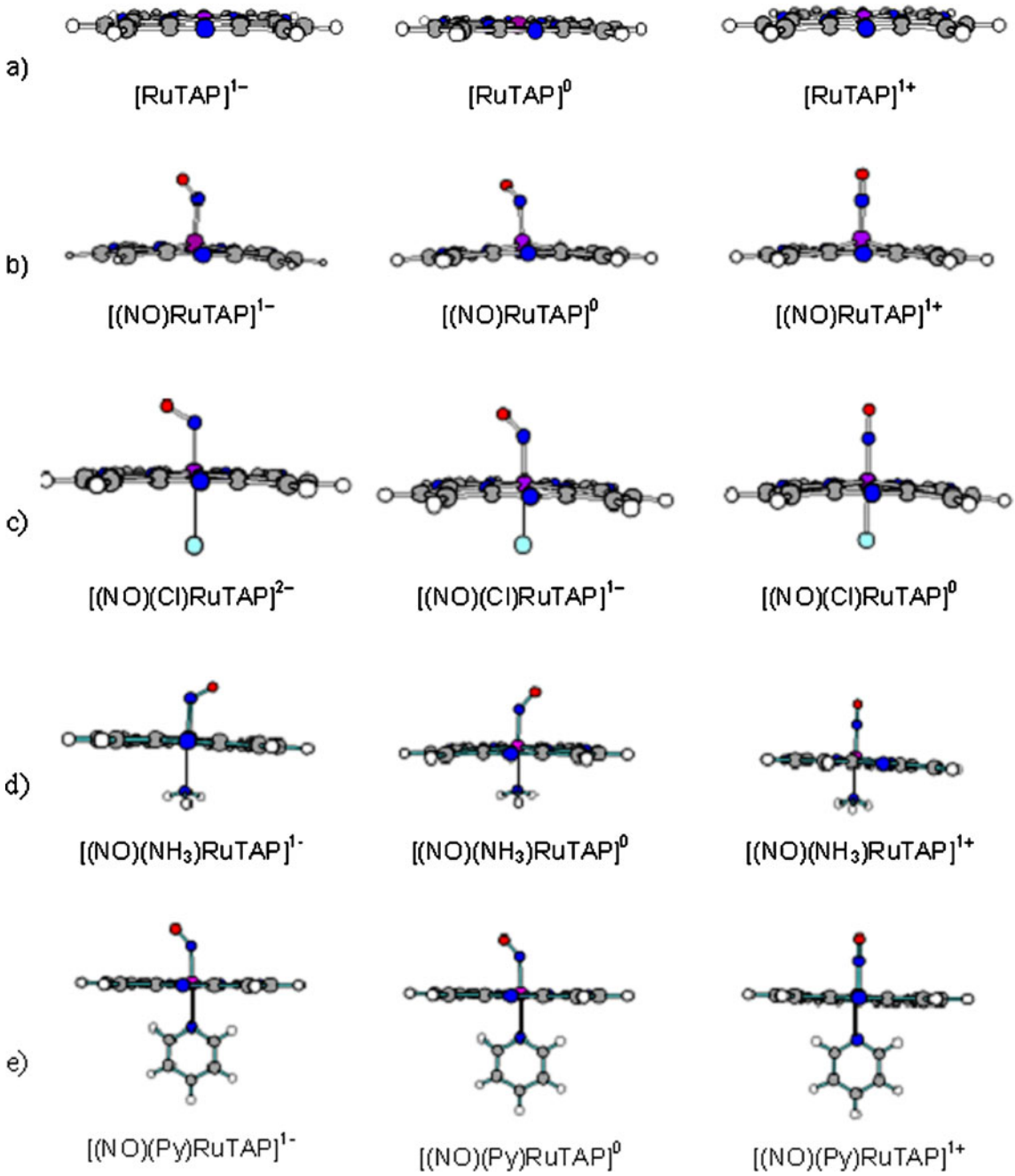

Fig. 2 Graphical representation of the molecular geometries fully optimized at B3LYP/6-31+G(d)/LANL2DZ level for all complexes studied

region between Ru and N of the NO group and as a result the Ru–N–O angle is linear.

As is well known, the bond order is a measure of the electronic density between two atoms and thus it stands for the bond strength. Increasing the bond order means increasing the electron density between atoms and, consequently, increasing the bond strength. As can be seen in Table 2, the oxidation process affects the bond order between Ru and N from NO (column BO_5 in Table 2). The values calculated using the NBO procedure at B3LYP/6-31+G(d)/LANL2DZ level for the +1, +2, and +3 oxidation states of Ru are 1.051, 1.129, and 1.881, respectively. As expected, these results agree with the calculated bond length discussed before, i.e., the $[Ru(NO)TAP]^{1-}$ complex that has the highest Ru–NO bond length also has the lowest bond order and the $[Ru(NO)TAP]^{1+}$ complex that has the lowest bond length also has the highest bond order. The atomic partial charges on Ru atom obtained from the CHELPG scheme are also affected by the oxidation-reduction processes. These charges range from +0.8 to +1.2, showing that the electron removed during the

Table 2 Bond orders (BO_x) calculated for selected bonds and atomic partial charges derived from CHELPG scheme for the Ru and NO groups. All values were obtained at B3LYP/6-31+G(d)/LANL2DZ level

Ru complex	Bond order							Atomic partial charge		
	BO_1	BO_2	BO_3	BO_4	BO_5	BO_6	BO_7	Ru	N^*	O
$[RuTAP]^{1-}$	0.463	0.463	0.463	0.463	———	———	———	0.5	——	——
$[RuTAP]^{0}$	0.428	0.428	0.428	0.428	———	———	———	1.4	——	——
$[RuTAP]^{1+}$	0.424	0.424	0.424	0.424	———	———	———	0.8	——	——
$[(NO)RuTAP]^{1-}$	0.438	0.477	0.497	0.438	1.051	1.796	——	0.8	−0.1	−0.2
$[(NO)RuTAP]^{0}$	0.437	0.427	0.457	0.437	1.129	1.797	———	1.1	−0.1	−0.1
$[(NO)RuTAP]^{1+}$	0.497	0.497	0.497	0.497	1.410	1.881	———	1.2	−0.1	0.0
$[(NO)Ru(Cl)TAP]^{2-}$	0.477	0.459	0.477	0.459	0.925	1.766	0.182	2.42	−0.54	−0.27
$[(NO)Ru(Cl)TAP]^{1-}$	0.454	0.444	0.452	0.446	0.891	1.778	0.387	2.25	−0.30	−0.18
$[(NO)Ru(Cl)TAP]^{0}$	0.449	0.449	0.449	0.449	1.276	1.912	0.502	2.15	−0.16	−0.05
$[(NO)Ru(NH_3)TAP]^{1-}$	0.473	0.454	0.472	0.455	0.931	1.809	0.129	2.04	−0.41	−0.24
$[(NO)Ru(NH_3)TAP]^{0}$	0.452	0.442	0.450	0.443	0.898	1.838	0.282	1.80	−0.16	−0.13
$[(NO)Ru(NH_3)TAP]^{1+}$	0.457	0.458	0.458	0.458	1.322	1.971	0.340	1.72	−0.07	0.02
$[(NO)Ru(Py)TAP]^{1-}$	0.430	0.450	0.472	0.452	0.953	1.809	0.099	1.86	−0.33	−0.26
$[(NO)Ru(Py)TAP]^{0}$	0.449	0.441	0.450	0.441	0.894	1.84	0.274	1.66	−0.06	−0.17
$[(NO)Ru(Py)TAP]^{1+}$	0.456	0.456	0.456	0.456	1.332	1.969	0.326	1.66	0.07	−0.03

$BO_1=N_6$–Ru, $BO_2=N_{14}$–Ru, $BO_3=N_{21}$–Ru, $BO_4=N_{29}$–Ru, BO_5=Ru–NO, $BO_6=N_{34}$–O_{35}, BO_7=Ru–L, where L=Cl^-, NH_3, or Py, and N^* stands for nitrogen from nitric oxide group

oxidation process comes almost entirely from the Ru atom, as expected. The charges on the N and O from NO group are slightly negative (see Table 2).

The binding energies (ΔE), enthalpies (ΔH) and Gibbs free energies (ΔG) of the complexation reactions are given in Table 3. A graphical visualization of ΔG for all complexation reactions is shown in Fig. 4. The analysis of the binding energies shows that the binding of NO to Ru(NO)TAP is energetically favorable for all oxidation states of Ru. It can be noted that BSSE and ZPVE corrections are very significant in the binding energy description, with variations around 15 $kcal\,mol^{-1}$ and 10 $kcal\,mol^{-1}$ for $[(NO)RuTAP]^{1+}$ and $[(NO)RuTAP]^{1-}$, respectively. The highest binding energy was calculated for the +2 state and the smallest for the +1 state of Ru. However, there is an inconsistency between the correlation of the binding energies with the bond order parameter. This inconsistency can be explained based on the definition of each parameter: the binding energy is calculated as the energy difference between products and reagents, while the bond order just concerns the electron density between adjacent atoms. So, the bond order does not take into consideration all possible contributions that the binding energy provides. It is expected that there is some correlation between the two parameters, but this is not mandatory. Additionally, in the porphyrin structure an anomalous behavior is expected, once again suggesting that this structure has a high electron correlation that impacts directly on the calculation of the energy of the molecular system. A better correlation with the binding energies should be made with Ru–NO bond length, since this is a parameter obtained through geometry optimization. However, the Ru(NO)TAP structures for the +2 and +1 oxidation states of Ru show weaker Ru–NO bonds with shorter bond length. This behavior can be explained by spin-orbit interactions and relativistic effects [44]. As can be seen in Table 3 and in Fig. 4, the enthalpies (ΔH) and the Gibbs free energies (ΔG) follow the same trend as binding energies with higher values than those observed for ΔE. In addition, Fig. 4 shows clearly that the ΔG from complexation reactions are all favorable and the most stable complex is observed when Ru is in its oxidation state +2.

In summary, we can postulate that the oxidation process affects the Ru–NO bonding in a systematic way, making it more labile in the +1 oxidation state of Ru and less labile for the +2 oxidation state of Ru. However, oxidation does not affect the TAP geometric and electronic parameters, which makes it suitable for use as a NO molecular carrier in a biological system.

Interaction between NO and Ru(Cl)TAP

This section aims to investigate the effect of axial chloride (Cl^-) ligand on the Ru–NO bond, as is shown in Fig. 3c. The chloride ion is −1 charged and the TAP is −2 charged, and therefore the resultant complex net charges are −2, −1, and 0 for the +1, +2, and +3, oxidation states of Ru, respectively, i.e., $[Ru(NO)(Cl)TAP]^{2-}$, $[Ru(NO)(Cl)TAP]^{1-}$, and [Ru

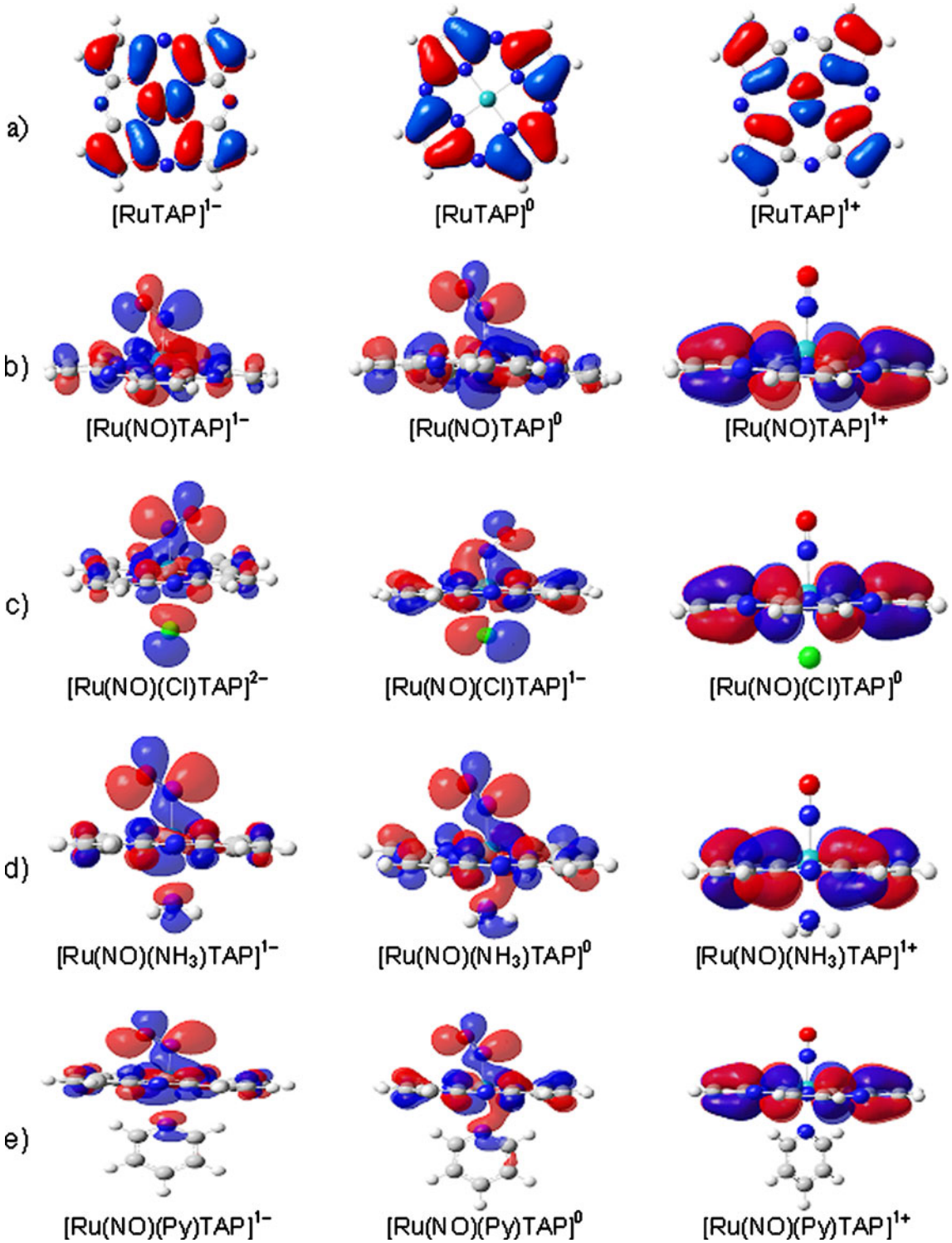

Fig. 3 Plot of the highest molecular orbital (HOMO) for the complexes studied. Observe that the HOMO orbital has no contribution from the Ru atom for the +3 oxidation state of Ru. This observation helps to explain the linear geometry found for the Ru–N–O angle

(NO)(Cl)TAP]^0. Table 4 shows that the Ru–Cl bond length is affected by the oxidation state of Ru. The calculated bond lengths are 2.824 Å, 2.511 Å, and 2.400 Å for the +1, +2, and +3 states of Ru, respectively. The Ru–Cl bond order (column BO_7 in Table 2) shows that this bond can be classified as a weak chemical bond, and the bond order increases with the increase in the oxidation state, i.e., the higher the oxidation state the higher the bond order.

Table 3 The binding energies (ΔE), enthalpies (ΔH) and Gibbs free energies (ΔG) for Ru–NO bond obtained according to the procedure described in Computational procedure section. ΔE and ΔE^{corr} stand for the binding energies without correction and with ZPVE and BSSE corrections, respectively. TAP has always charge −2. All values are given in kcal/mol

	Complexation reaction	ΔE	$\Delta E^{BSSE+ZPVE}$	ΔH	ΔG
a1)	$[RuTAP]^{1-} + NO \rightarrow [(NO)RuTAP]^{1-}$	−34.05	−24.77	−24.12	−11.50
a2)	$[RuTAP]^{0} + NO \rightarrow [(NO)RuTAP]^{0}$	−59.04	−59.67	−58.83	−46.67
a3)	$[RuTAP]^{1+} + NO \rightarrow [(NO)RuTAP]^{1+}$	−59.65	−44.51	−40.79	−27.21
b1)	$[Ru(Cl)TAP]^{2-} + NO \rightarrow [(NO)Ru(Cl)TAP]^{2-}$	−37.84	−28.45	−27.26	−15.74
b2)	$[Ru(Cl)TAP]^{1-} + NO \rightarrow [(NO)Ru(Cl)TAP]^{1-}$	−35.11	−28.26	−27.02	−16.57
b3)	$[Ru(Cl)TAP]^{0} + NO \rightarrow [(NO)Ru(Cl)TAP]^{0}$	−63.98	−41.78	−39.62	−27.49
c1)	$[Ru(NH3)TAP]^{1-} + NO \rightarrow [(NO)Ru(NH3)TAP]^{1-}$	−33.49	−26.43	−24.60	−14.44
c2)	$[Ru(NH3)TAP]^{0} + NO \rightarrow [(NO)Ru(NH3)TAP]^{0}$	−34.72	−30.41	−28.69	−19.89
c3)	$[Ru(NH3)TAP]^{1+} + NO \rightarrow [(NO)Ru(NH3)TAP]^{1+}$	−64.74	−58.69	−55.69	−44.67
d1)	$[Ru(Py)TAP]^{1-} + NO \rightarrow [(NO)Ru(Py)TAP]^{1-}$	−33.04	−25.99	−25.32	−11.81
d2)	$[Ru(Py)TAP]^{0} + NO \rightarrow [(NO)Ru(Py)TAP]^{0}$	−33.48	−28.77	−27.47	−16.90
d3)	$[Ru(Py)TAP]^{1+} + NO \rightarrow [(NO)Ru(Py)TAP]^{1+}$	−61.57	−54.23	−50.25	−38.15

The presence of the chloride ion ligand increases the Ru–NO bond length. This increase is about 1 % for the +1 state, 3.5 % for the +2 state, and 2.4 % for the +3 state of Ru. The Ru–NO bond order is quite affected by the chloride ion ligand at axial position. As shown in Table 2, the decreases in bond order are 0.93 %, 21.0 %, and 9.5 %, for the +1, +2, and +3 states of Ru, respectively, when compared to Ru (NO)TAP for equivalent states. These results are closely related to the bond length's decrease and show clearly that the chloride ion ligand in axial position affects the Ru–NO bond, and this effect is more pronounced for the +2 state of Ru. The binding energies in Table 3 show that the bonding between the NO group and the $[Ru(Cl)TAP]^{2-}$, $[Ru(Cl)TAP]^{1-}$, and $[Ru(Cl)TAP]^{0}$ complexes are all energetically favorable. However, the binding energy between NO and $[Ru(Cl)TAP]^{0}$ is about 48 % greater than the binding energy for NO bonded to $[Ru(Cl)TAP]^{1-}$, which has the smallest binding energy. The BSSE and ZPVE corrections are also very significant in the binding energy calculation, with variations around 20 kcalmol^{-1} and 7 kcalmol^{-1} for $[(NO)Ru(Cl)TAP]^{0}$ and $[(NO)Ru(Cl)TAP]^{-1}$, respectively. The (NO)Ru(Cl)TAP structures for +1 and 0 oxidation states of Ru show weaker Ru–NO bonds with shorter bond length. This behavior for binding energies follows the same trend as that in results discussed for Ru(NO)TAP. However, the Gibbs free energies (ΔG) in Table 3 and in Fig. 4 show that the $[Ru(Cl)TAP]^{1-}$ complex is slightly more stable than the $[Ru(Cl)TAP]^{2-}$ complex and the $[Ru(Cl)TAP]^{0}$ is the most stable complex.

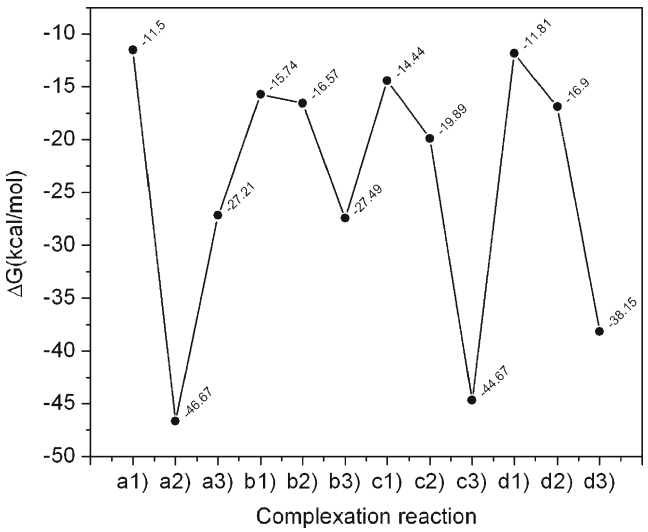

Fig. 4 Graphical representation of Gibbs free energies (ΔG) for the complexation reactions according to Table 3. All values are given in kcalmol^{-1}

As can be seen in Table 4 and Fig. 2c the Ru–N–O angle bends for the $[Ru(NO)(Cl)TAP]^{2-}$ and $[Ru(NO)(Cl)TAP]^{1-}$ complexes, while it is linear for $[Ru(NO)(Cl)TAP]^{0}$. These values are similar to those calculated for the Ru(NO)TAP complexes, in which the Ru has equivalent oxidation state. Again, the explanation can be found in the HOMO nature (see Fig. 3c). The chloride ion ligand has no effect on N–O bond from NO group, as can be seen in Tables 1 and 4. The projection of Ru atom out of the molecular plane is very small and it is projected in the direction of the NO group. It is more pronounced when the oxidation state of the Ru atom is +3. In this state the Ru–NO bond length is shorter and the Ru–N–O angle is linear.

In summary, the geometric and electronic parameters of the Ru–NO bond are quite noticeably affected by the presence of the chlorine ion ligand and the oxidation state of the [(NO)Ru(Cl) TAP] complex, and the Ru–NO bond is more labile for the +1 oxidation state of Ru.

Interaction between NO and $Ru(NH_3)TAP$

As is known, ammonia (NH_3) is an uncharged chemical compound that can act as a ligand in transition metal complexes; it has been explored in designing new compounds to be used in biological systems [8, 17]. Our aim in this section

Table 4 Bond lengths (Å) and bond angles (°) calculated for Ru(NO)(L)TAP (L=Cl^-, NH_3, or Py) complexes with oxidation state of Ru ranging from +1 to +3 at the B3LYP/6-31+G*/LANL2DZ level

	Ru^{1+} [(NO)Ru (Cl)TAP]$^{2-}$	Ru^{2+} [(NO)Ru (Cl)TAP]$^{1-}$	Ru^{3+} [(NO)Ru (Cl)TAP]^{0}	Ru^{1+} [(NO)Ru (NH_3)TAP]$^{1-}$	Ru^{2+} [(NO)Ru (NH_3)TAP]^{0}	Ru^{3+} [(NO)Ru (NH_3)TAP]$^{1+}$	Ru^{1+} [(NO)Ru (Py)TAP]$^{1-}$	Ru^{2+} [(NO)Ru (Py)TAP]^{0}	Ru^{3+} [(NO)Ru (Py)TAP]$^{1+}$
N6 – Ru	1.999	2.010	2.021	2.002	2.011	2.019	2.002	2.011	2.017
N14 – Ru	2.010	2.016	2.021	2.013	2.018	2.019	2.014	2.016	2.018
N21 – Ru	1.999	2.010	2.021	2.002	2.012	2.019	2.000	2.011	2.017
N29 – Ru	2.010	2.016	2.021	2.013	2.017	2.019	2.011	2.016	2.018
Ru – NO	1.941	1.890	1.770	1.944	1.892	1.764	1.944	1.894	1.761
Ru – plane	0.038	0.044	0.078	0.103	0.108	0.211	0.098	0.062	0.161
N – O	1.220	1.190	1.157	1.212	1.181	1.149	1.211	1.181	1.149
N21 –Ru–N14	179.74	177.22	179.97	174.08	173.87	168.00	174.37	176.47	170.8
Ru–N–O	121.59	139.93	179.95	120.55	139.54	180.00	120.08	139.22	180.0
Ru – Cl	2.824	2.511	2.400	———	———	———	———	———	———
Ru – NH3	———	———	———	2.518	2.257	2.209	———	———	———
Ru – Py	———	———	———	———	———	———	2.628	2.274	2.242

was to investigate if NH_3 can bind to the Ru atom in the axial position to form the [(NO)Ru(NH_3)TAP] complex and analyze the effects of the NH_3 ligand on the geometric and electronic parameters of the Ru–NO bond. As usual, the TAP has charge −2 and we considered the +1, +2, and +3 oxidation states of Ru, forming the following complexes: [(NO)Ru(NH_3)TAP]$^{1-}$, [(NO)Ru(NH_3)TAP]^{0}, and [(NO)Ru (NH_3)TAP]$^{1+}$.

The geometric parameters fully optimized for the [(NO)Ru(NH_3)TAP] complex at B3LYP/6-31+G(d)/LANL2DZ level are described in Table 4 and in Fig. 2d. The calculation results show that the Ru–NH_3 bond length is also affected by the oxidation state of Ru. The bond lengths of 2.518 Å, 2.257 Å, and 2.209 Å for the +1, +2, and +3 oxidation states of Ru, respectively, are about 12 % lower than those obtained for the Ru–Cl bond length in the equivalent oxidation state of Ru. The Ru–NH_3 bond orders for all three oxidation states can be classified as weak bonds, and the calculated values are 41 %, 37 %, and 47 % lower than those obtained for the Ru–Cl bond in the same state of Ru. The projection of the Ru atom out of the molecular plane when the NH_3 ligand is bonded at axial position are 0.103 Å, 0.108 Å, and 0.211 Å for the +1, +2, and +3 states of Ru, respectively. These values are about 171 %, 145 %, and 170 % greater than the values calculated for [(NO)Ru(Cl)TAP] complexes in the equivalent oxidation states. This effect can be understood considering that NH_3 is a weaker ligand than the Cl^- ion.

The results in Table 3 show that Ru–NO binding energies, enthalpies and Gibbs free energies for the [(NO)Ru (NH_3)TAP] complexes are all favorable to complex formations and they are greatly affected by the oxidation state of Ru. The BSSE and ZPVE corrections are less significant in the description of the binding energies when compared with the previous structures with variations around 7 kcal mol^{-1}. These complexes did not show the behavior observed in the [Ru(NO)TAP] and [(NO)Ru(Cl)TAP] structures, i.e., weaker Ru–NO bonds with shorter bond length. This is explained due the strong activating character of the NH_3 group, which makes up for the lack of electrons in the structure because of the oxidation. For the +3 state of Ru, the Ru–NO binding energy in [(NO)Ru(NH_3)TAP]$^{1+}$ complex is about 40 % greater than Ru–NO binding energy in [(NO)Ru(NH_3)TAP]^{0} complex and about 39 % greater than Ru–NO binding energy in [(NO)RuTAP]$^{1+}$. The binding energies for +1 and +2 states of Ru are similar to those obtained for [(NO)Ru(Cl)TAP] and [(NO)RuTAP] complexes for the same oxidation state of Ru. The only exception is for [(NO)RuTAP]^{0}, which presents a Ru–NO binding energy of 59.67 kcal mol^{-1}. The Ru–N–O bending angles for [(NO)Ru(NH_3)TAP] complexes are similar to those calculated for [(NO)Ru(Cl)TAP] complexes considering equivalent oxidation states of Ru. The N–O bond lengths for [(NO) Ru(NH_3)TAP] complex in the +1 and +2 oxidation states of Ru are very similar to the values calculated for [(NO) RuTAP] and [(NO)Ru(Cl)TAP] for equivalent oxidation states of Ru. However, for the +3 oxidation state of Ru there is a slight decrease in the N–O bond length.

In summary, the NH_3 ligand in the axial position affects the geometric, electronic, and energetic parameters of the Ru–NO bond in the Ru(NO)(NH_3)TAP complex when compared to [(NO)RuTAP] for all equivalent oxidation states of Ru. The geometric and electronic parameters of the Ru–NH_3 bond are also affected by the oxidation state of Ru. In addition, the geometric and electronic parameters of the TAP are not affected by the NH_3 ligand.

Interaction between NO and Ru(Py)TAP

Pyridine (Py) is a basic heterocyclic organic compound which is a relatively weak ligand in forming complexes with transition metal ions. In this section we describe the calculation results of the effect of pyridine ligand at axial position on the geometric and electronic parameters of the Ru–NO bond (see Fig. 2e). Again, the TAP ligand is −2 charged and Py is an uncharged ligand. Therefore, for the +1, +2, and +3 oxidation states of Ru, we have the [(NO)Ru(Py)TAP]$^{1-}$, [(NO)Ru(Py)TAP]^{0}, and [(NO)Ru(Py)TAP]$^{1+}$, complexes, respectively. The calculated values for Ru–Py bond length are 2.628 Å, 2.274 Å, and 2.242 Å for the +1, +2, and +3 oxidation states of Ru, respectively. These values are situated between those obtained for [(NO)Ru(NH_3)TAP] and [(NO)Ru(Cl)TAP] complexes for equivalent oxidation states of Ru. The calculated Ru–Py bond orders for the +1, +2, and +3 oxidation states of Ru (see column BO_7 in Table 2) show that those bonds can be considered as weak chemical bonds, and they are slightly smaller than those observed for Ru–NH_3 in the [(NO)Ru(NH_3)TAP] complexes considering equivalent oxidation states of Ru. The effects of the Py ligand at the axial position on the Ru–N–O angle and on Ru–NO and N–O bond lengths in the [(NO)Ru(Py)TAP] complexes are equivalent to those obtained for [(NO)Ru(NH_3)TAP] complexes. The Ru projections out of the molecular plane in the [(NO)Ru(Py)TAP] complexes are slightly smaller than those values observed for [(NO)Ru(NH_3)TAP] complexes in the equivalent oxidation states of Ru. The effect of the Py ligand on the Ru–NO bond orders in the [(NO)Ru(Py)TAP] complexes are also equivalent to those observed for [(NO)Ru(NH_3)TAP] complexes for all the three states studied. The Ru–NO binding energies, enthalpies and Gibbs free energies in Table 3 for [(NO)Ru(Py)TAP] complexes show that the NO complexation to Ru(Py)TAP complex is energetically favorable for the +1, +2, and +3 states of Ru and are a little smaller for those obtained in the [(NO)Ru(NH_3)TAP] complexes for equivalent oxidation state: This is explained by the strong activating character of the pyridine group, which makes up for the lack of electrons in the structure because of the oxidation state. Similar to the [(NO)Ru(NH3)TAP] structure, the BSSE and ZPVE corrections are less significant in the description of the binding energies, with variations around 7 kcalmol^{-1}.

In summary, the Py axial ligand affects the geometric and electronic parameters of the Ru–NO bond, but does not affect the geometric and electronic parameters of TAP and the N–O bond. These effects are similar to those observed in [(NO)Ru(NH_3)TAP] complexes. In addition, the geometric and electronic parameters of the Ru–Py bond are also dependent on the oxidation state of Ru.

Conclusions

The results of the calculation carried out on RuTAP, [(NO)RuTAP], [(NO)Ru(L)TAP] (L=Cl^-, NH_3, Py) complexes for the +1, +2, and +3 oxidation states of Ru at B3LYP/6-31+G(d)/LANL2DZ level show that the Ru–NO bond is energetically stable and the binding energies are highly dependent on the oxidation state of Ru and on the chemical nature of the L ligand. The geometric parameters and the bond orders of the Ru–NO bond are also highly dependent on the oxidation state of Ru and of the L ligand. An interesting fact is that the geometric parameters of the TAP ligand do not depend on the +1, +2, and +3 oxidation states of Ru and L ligand studied. This means that the TAP ligand should keep its characteristic chemical stability in the complexes. These theoretical results show that the [(NO)RuTAP], [(NO)Ru(L)TAP] complexes are good candidates for use as nitric oxide carriers in living organisms. Having selected the biological target of interest one can then select an appropriate L ligand and an appropriate oxidation state of Ru to design a specific NO carrier. Furthermore, different behavior for the [Ru(NO)TAP] and [(NO)Ru(Cl)TAP] structures was observed: weaker Ru–NO bonds with shorter bond length. This behavior is not observed for the [(NO)Ru(NH_3)TAP] and [(NO)Ru(Py)TAP] structures, because these substituents (NH_3 and Py) have a strong activating character that makes up for the lack of electrons in the structure because of the oxidation.

Acknowledgments The authors gratefully acknowledge the support given to this work by grants from Unidade Universitária de Ciências Exatas e Tecnológicas (UnUCET) of the Universidade Estadual de Goiás (UEG) and FINATEC, the Brazilian Foundation for Scientific and Technological Enterprises.

References

1. Battino R, Clever HL (1966) Chem Rev 66:395–463
2. Wilhelm E, Battino R, Wilcock RJ (1977) Chem Rev 77:219–262
3. Wang PG, Xian M, Tang MX, Wu X, Wen Z, Cai T, Janczuk AJ (2002) Chem Rev 102:1091–1134
4. Feelish M, Stamler JS (eds) (1996) Methods in nitric oxide research. Wiley, Chichester
5. Cooper CE (1999) Biochim Biophys Acta 290:1411–1418
6. Ford PC, Bourassa J, Miranda K, Lee B, Lorkovic I, Boggs S, Kudo S, Laverman L (1998) Coord Chem Rev 171:185–202
7. Stochel G, Wanat A, Kulis E, Stasicka Z (1998) Coord Chem Rev 171:203–220
8. Toledo JC Jr, Lopes LGF, Alves AA, Silva LP, Franco DW (2002) J Inorg Biochem 89:267–271
9. Benini PGZ, da Silva JJN, Osakabe AL, Silva JS (2006) Nitric Oxide-Biology Chem 14:A53–A54
10. Venturini G, Salvati L, Muolo M, Colasanti M, Gradoni L, Ascenzi P (2000) Biochem Biophy Res Commun 270:437–441
11. Queiroz SL (1999) Quím Nova 22:584–590

12. Feldman PL, Griffith OW, Stuehr DJ (1993) Chem Eng News 71:26–38
13. Furchgott RF, Zawadzki JV (1980) Nature 288:373–376
14. Kurtikyan TS, Ford PC (2008) Coord Chem Rev 252:1486–1496
15. Rawlins WT, Person JC, Fraser ME, Miller SM, Blumberg WAM (1998) J Chem Phys 109:3409–3417
16. Kelm M, Schrader J (1990) Circ Res 66:1561–1575
17. Carlos RM, Cardoso DR, Castellano EE, Osti RZ, Camargo AJ, Macedo LG, Franco DW, Am J (2004) Chem Soc 126:2546–2555
18. DeLeo MA, Ford PC (2000) Coord Chem Rev 208:47–62
19. Cheng L, Movozhilova I, Kim C, Kovalevsky A, Bagley KA, Coppens P, Richter-Addo GB (2000) J Am Chem Soc 122:7142–7143
20. Works CF, Jocher CJ, Bart GD, Bu X, Ford PC (2002) Inorg Chem 41:3728–3739
21. Bohle DS, Hung CH, Smith BD (1998) Inorg Chem 37:5798–5806
22. Allardyce CS, Dyson PJ (2001) Platinum Met Rev 45:62–69
23. Richards AD, Rodger A (2007) Chem Soc Rev 36:471–483
24. Toledo JC, Silva HA, Scarpellini M, Miori V, Camargo AJ, Bertotti M, Franco DW (2004) Eur J Inorg Chem 9:1879–1885
25. Caramori G, Frenking G (2007) Organometallics 26:5815–5825
26. Gaussian 03, Revision C.02, Frisch MJ et al (2004) Gaussian, Inc., Wallingford CT
27. Becke AD (1993) J Chem Phys 98:5648–5652
28. Lee C, Yang W, Parr RG (1988) Phys Rev B 37:785–789
29. Miehlich B, Savin A, Stoll H, Preuss H (1989) Chem Phys Lett 157:200–206
30. Kestner NR (1968) J Chem Phys 48:252–257
31. Salvador P, Simon S, Duran M, Dannenberg JJ (2000) J Chem Phys 113:5666–5673
32. Boys SF, Bernardi F (1970) Mol Phys 19:553–566
33. Foster JP, Weinhold F (1980) J Am Chem Soc 102:7211–7218
34. Reed AE, Weinhold F (1983) J Chem Phys 78:4066–4073
35. Reed AE, Weinstock RB, Weinhold F (1985) J Chem Phys 83:735–746
36. Reed AE, Weinhold F (1985) J Chem Phys 83:1736–1740
37. Carpenter JE (1987) Extension of Lewis structure concepts to open-shell and excited-state molecular species, Ph. D. thesis, University of Wisconsin, Madison, WI
38. Carpenter JE, Weinhold F (1988) J Mol Struct 46:41–62
39. Reed AE, Curtiss LA, Weinhold F (1988) Chem Rev 88:899–926
40. Glendening ED, Reed AE, Carpenter JE, and Weinhold F, NBO, Version 3.1.
41. Breneman CM, Wiberg KB (1990) J Comp Chem 11:361–373
42. Sedano PS (2001) Implementation and application of basis set superposition error-correction schemes to the theoretical modeling of weak intermolecular interactions. Dissertation of Doctor in Philosophy, University of Girona, Girona
43. McQuarrie DA, Simon JD (1997) Physical Chemistry: A Molecular Approach. University Science, Sausalito
44. Kraka E, Cremer D (2012) Proc Quím 6:31–34